Supplementary Information

Highly conductive low-temperature combustion-derived transparent indium tin oxide thin film

Longfei Song,[1,2] Tony Schenk,[1] Emmanuel Defay,[1] Sebastjan Glinsek[1]*

1. Materials Research and Technology Department, Luxembourg Institute of Science and Technology, rue du Brill 41, L-4422 Belvaux, Luxembourg. E-mail: longfei.song@list.lu

2. University of Luxembourg, 41 rue du Brill, L-4422 Belvaux, Luxembourg

1. Williamson-Hall Method

Williamson-Hall (W-H) method was used to characterize the crystalline domain size *D* (i.e. size of coherently diffracting domains) and the lattice microstrain ε in our films (i.e. distribution of interplanar spacings arising from strain fields caused by defects in the lattice)[1]. Scherrer equation links crystallite size D with the integral breath β_D of the diffracted peak:

$$D = \frac{K_D \lambda}{\beta_D \cos\theta} \quad (1)$$

, where K_D is Scherrer constant (0.94), λ is wavelength of the X-rays (1.5406 Å) and θ is the diffraction angle. On the other hand, microstrain can be defined as:

$$\varepsilon = \frac{\beta_s}{2K_s \tan\theta} \quad (2)$$

, where K_s is the proportionality constant (2 was used in this case).[2-3] Note that the influence of *D* and ε on the width of diffracted peaks can be separated based on their dependence of diffraction angle, i.e. inverse of cosθ and tanθ for *D* and ε, respectively.

Size- and microstrain related broadening of the diffraction peaks add to the integral breath of the peak β_{hkl}:

$$\beta_{hkl} = \beta_D + \beta_s \quad (3)$$

Combining Equations (1), (2) and (3) one gets:

$$\beta_{hkl} = \frac{K_D \lambda}{D \cos\theta} + \varepsilon 2K_s \tan\theta \quad (4)$$

, and by multiplying all sides of Equation (4) with cosθ:

$$\beta_{hkl} \cos\theta = \frac{K_D \lambda}{D} + \varepsilon 2K_s \sin\theta \quad (5)$$

The β_{hkl} values were obtained from fitting the peaks in Figure 2a in the main manuscript with Lorentzian function using Jade 6.0 software. Using equation (5), $\beta_{hkl}\cos\theta$ of different peaks observed in Fig. 2a in the

main manuscript is plotted as a function of 4sinθ for the films prepared form different solution concentration in Fig. S1. By linearization, crystallite size D was obtained from the intercept and microstrain ε from the slope. Results of the fitting are shown in Table S1.

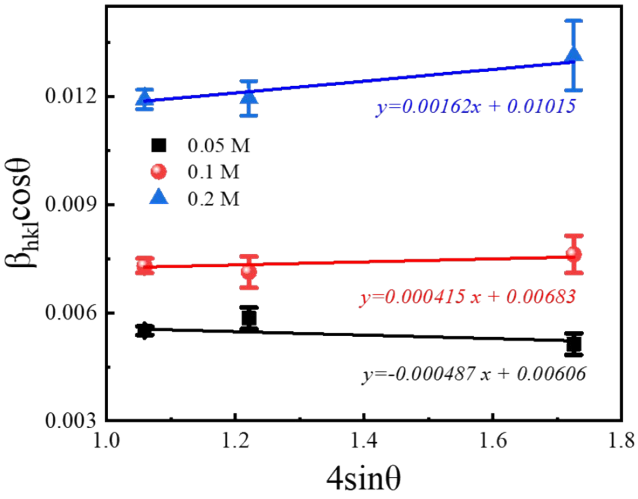

Fig S1 W-H analysis (β_{hkl} cosθ as a function of 4sinθ) of the ITO films prepared from solutions with different concentrations (0.05, 0.1 and 0.2 M). Symbols are experimental data, lines are linear fits.

Table S1: Results of the linear fits shown in Fig S1 using Equation (5).

Sample	0.05 M-ITO	0.1 M-ITO	0.2 M-ITO
Slope (x 10^{-3})	-0.487	0.415	1.62
Intercept (x10^{-3})	6.06	6.83	10.15
D (in nm)	22.9	20.3	13.6
ε (x10^{-3})	-0.48	0.42	1.6

2. AFM Experiments

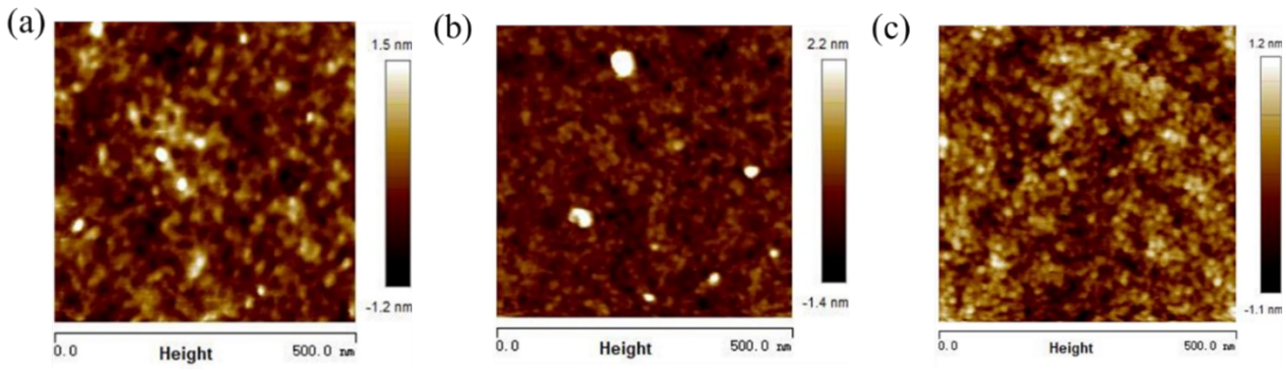

Fig S2 AFM images showing surface of the ITO films prepared from: (a) 0.05 M solution, (b) 0.1 M solution,

(c) 0.2 M solution .

2. Tilt angle ψ dependent GIXRD Measurements

Tilt-angle dependent XRD measurements were performed in order to measure biaxial stress in our ITO samples. Due to the film thickness of only 50 nm, symmetric θ-2θ scans were not sensitive enough. Therefore, a grazing incidence approach was used with a constant incidence angle α = 1°. Subsequent 2θ scans were performed for the 222 peak in 2θ steps of 0.02° for different angles Ψ_d along the Eulerian cradle of the diffractometer. In the symmetric θ-2θ configuration, Ψ_d would be equal to the tilt angle Ψ of the scattering vector toward the surface normal of the film as indicated in Fig. S3. The resulted peak shifts of XRD patterns were shown in Fig. S4. In our non-symmetric α-2θ scans, α gives rise to an additional tilt-component. A correction needs to be applied and Ψ is given by:

$$\cos(\Psi) = \cos(\theta - \alpha) \cdot \cos(\Psi_d) \qquad (6)$$

No further corrections such as refraction, Lorentz polarization or absorption correction were used as this level of detail is beyond the scope of the present work. A Pseudo-Voigt function was used to fit the peak profiles and the resulting peak positions $\theta_{222}(\Psi)$ were used to calculate the corresponding lattice plane spacings $d_{222}(\Psi)$ from Bragg's law. These tilt-angle dependent lattice plane spacings were plotted vs. $\sin^2(\Psi)$ in Fig 2c to derive in-plane and out-of-plane strains (without the need of a standard for the strain-free lattice plane spacing d_0) as explained elsewhere. The obtained data for rotational-symmetric in-plane strain ε_{11}, plane-normal strain ε_{33}, and the corresponding stress components σ_{11}, and σ_{33} are detailed in Table S2, respectively, using a Poisson ratio of 0.35 and Young's modulus of 116 GPa.[4] The whole calculation process can be found in the previous report.[5]

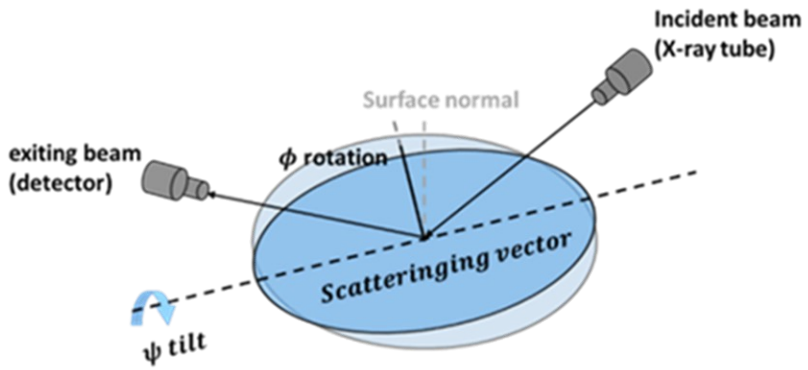

Fig S3 Sketch of changing the sample orientation relative to the scattering vector via Φ rotations and Ψ tilts (see methods section).

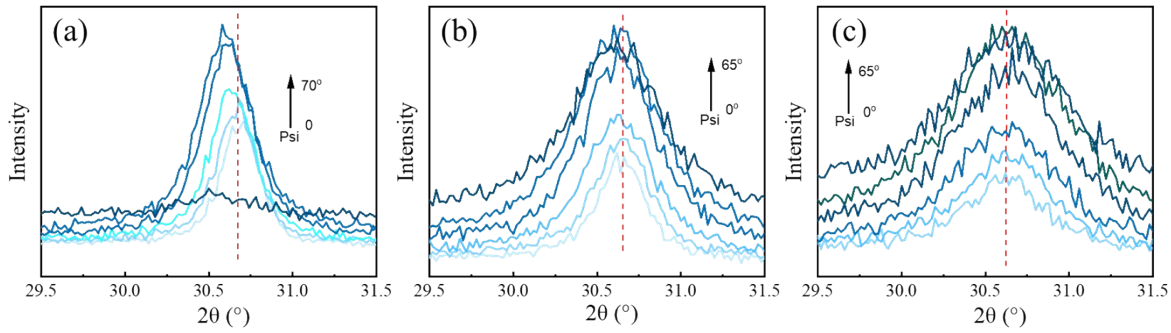

Fig S4 Peak shift of GIXRD patterns by varying Ψ-tilts at fixed Φ, (a) 0.05 M-ITO, (b) 0.1 M-ITO, (c) 0.2 M-ITO.

Table S2: Calculated strain and stress in ITO thin films prepared by using different solution concentration. In these calculation, Yong's modulus Y is 116 GPa, and Poisson's ratio ν is 0.35.[4] The whole calculating process is detailed indicated in the previous report. [5]

Y in GPa	**116**	**116**	**116**
ν	**0.35**	**0.35**	**0.35**
	222 Peak ($2\theta \approx$ 30.6 °)		
Sample	**0.05 M-ITO**	**0.1 M-ITO**	**0.2 M-ITO***
Slope (m) in pm	1.3125	0.4229	-0.2584
Intercept (n) in pm	290.95	291.34	291.65
d_0 in pm	291.63	291.56	291.52
$\varepsilon_{11}=\varepsilon_{22}$ in %	0.22	0.07	-0.04
ε_{33} in %	-0.23	-0.08	0.05
$\sigma_{11}=\sigma_{22}$ in MPa	390	120	-80
σ_{33} in GPa	0.00	0.00	0.00
dV/V_0	0.20	0.06	-0.04

*Due to large scattering of the experimental data the negative sign of strain and stress values is not reliable.

References:

[1] M. Birkholz, Thin Film Analysis by X-Ray Scattering, 2016.

[2] A. Khorsand ZakW.H. Abd. MajidM.E. AbrishamiRamin Yousefi, Solid State Sciences, 2011, **13**, 251-256.

[3] P. M. Kibasomba, S. Dhlamini, M. Maaza, C. P. Liu, M. M. Rashad, D. A. Rayan, B. W. Mwakikunga, Results in Physics, 2018, **9**, 628-635.

[4] B.-K. Lee, Y.-H. Song, J.-B. Yoon, Indium Tin Oxide (ITO) Transparent MEMS Switches, 2009 IEEE 22nd International Conference on Micro Electro Mechanical Systems, Sorrento, Italy.

[5] T. Schenk, C. M. Fancher, M. H. Park, C. Richter, C. Künneth, A. Kersch, Jacob L. Jones, T. Mikolajick and U. Schroeder, Origin of the Large Remanent Polarization in La:HfO_2. Adv. Electron. Mater., 2019, **12**, 1900303.